Upsala J Med Sci 77: 67–76, 1972

Resistance Kinetics following Convection-Velocity Steps in the Teorell Membrane Oscillator

JARL V. HÄGGLUND

Institute of Physiology and Medical Biophysics, The Biomedical Centre, Uppsala, Sweden

ABSTRACT

The kinetic behaviour of the resistance in Teorell's membrane oscillator has been subjected to theoretical analysis. A membrane model has been considered which takes into account convection and diffusion as transport mechanisms. The nonlinear time dependence of the membrane resistance has been calculated for a step function in the convection velocity. The exact solution has been compared with Teorell's monoexponential approximation of the resistance-decay function. The implications of the more complete convection-diffusion model are discussed and a modified expression of the rate constant is suggested. The results of the investigation are relevant when the membrane oscillator is used as a model of biological excitable cells.

INTRODUCTION

Oscillations in artificial membranes have attracted much attention as models of oscillatory behaviour in living cells. Teorell (1) first showed the existence of sustained oscillations of the electric potential in a porous membrane with fixed charges separating two electrolyte solutions with different concentrations. Hydrostatic pressure and electro-osmosis with accompanying bulk-flow (i.e. convection) played an essential part in the origin of the oscillations. Rhythmic variations in the bulk-flow velocity and the pressure, as well as in the membrane resistance, accompanied the electric potential oscillations. The energy for the oscillations was supplied by a constant current applied across the membrane.

A theoretical description of the oscillations was also given by Teorell (2). The periodic changes in the resistance were associated with variations in the concentration profile caused by the periodic changes in the bulk-flow velocity. An essential feature of Teorell's theory is the time-delay function of the resistance, due to changes in the convection velocity. Without this delay function, no oscillations will occur. The physical basis for the resistance delay is the relaxation of the concentration profile, which is dependent on the combined action of convection and diffusion. Teorell introduced an approximation in the form of a first-order differential equation with respect to time, expressing the rate of change of the resistance as proportional to the deviation of the instantaneous resistance from the steady-state value. This approximation was found to be satisfactory, though the exact expression of the instantaneous resistance is certainly a much more complex function, as Teorell pointed out.

Other investigators have used different approaches to explain Teorell's membrane oscillator. Kobatake & Fujita (3) have formulated a theory based on a thermodynamic and hydrodynamic treatment. Aranow (4) has studied the hydrodynamic stability of the membrane oscillator. The different theories proposed for Teorell's membrane oscillator have been reviewed and compared by Caplan & Mikulecky (5). All the theories include approximations, but Teorell's formulation has the advantage of being especially suitable for the successful simulation of a number of important biological phenomena in excitable tissue (6). Aranow (7) has also succeeded in verifying Teorell's approximation of the instantaneous resistance, using a perturbation technique. However, her treatment is only valid for a linear case, and is thus an approximation of a more general non-linear behaviour.

The purpose of the present paper is to investigate a more complete model of the time-delay function of the resistance in Teorell's excitability analogue. The model used is based on convection and diffusion as mechanisms of the concentration profile relaxation. The time dependence of the resistance, caused by changes in the convection velocity, has been analysed. In other words, the input–output relations of the convection-diffusion model have been studied with the convection velocity as the input variable and the membrane resistance as the output variable. Following the methods of control-system theory, there are two main possibilities of describing the system which are relevant in the pres-

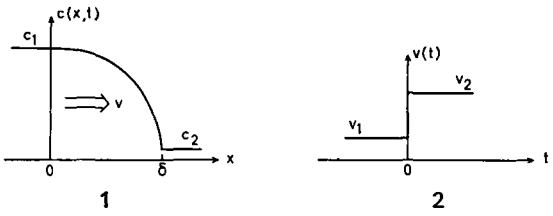

Fig. 1. The convection-diffusion membrane model. The membrane extends from 0 to δ in the x direction. The exterior salt solutions have the constant concentrations c_1 and c_2 respectively. The ions in the membrane are transported by diffusion and convection (i.e. solvent drag) with the velocity v.

Fig. 2. The step function in the convection velocity v from a value v_1 to a new value v_2. When the velocity step is applied to the membrane model in Fig. 1, the concentration profile changes, thus causing a transient relaxation of the membrane resistance.

ent case: (*a*) transient input response, and (*b*) frequency and phase response due to a periodic input. Frequency analysis for non-linear systems will be complicated by the fact that each input frequency will correspond to an output frequency spectrum. This investigation has been restricted to *a study of the time-dependence of the resistance due to a step function in the convection velocity*. The results are of importance for the kinetic description of the membrane oscillator and have proved to be especially essential for the simulation of biological voltage-clamp experiments (8). The equations used constitute a formal analogy to a constant-field single-ion electrodiffusion system (9). Thus the present analysis is of interest also in connection with electrodiffusion models for understanding the behaviour of excitable cells.

THEORY

A porous membrane of thickness δ is considered; it separates two compartments containing a salt solution at different concentrations c_1 and c_2 (Fig. 1). The pores are assumed to be wide, so that interaction with the pore walls can be neglected. The transport mechanisms are diffusion with the diffusion coefficient D and convection, i.e. bulk-flow or solvent drag, with the linear velocity v. The one-dimensional problem is considered with variations in the space dimension x parallel to the diffusion-convection pathway. The non-steady-state properties of this membrane model are analysed, allowing variations as a function of time t. If the concentration inside the membrane is $c(x, t)$, then the integral instantaneous resistance $r(t)$ (Ω cm^2) of the membrane is given by (10, 2, 5)

$$r(t) = \int_0^\delta \frac{dx}{\lambda c(x,t)} \tag{1}$$

where λ is a constant describing the electrical behaviour of the salt solution. For a monovalent salt (10)

$$\lambda = F^2(u_+ + u_-), \tag{2}$$

where u_+ is the molar mobility of the cation (cm^2 mole/joule sec), u_- is the molar mobility of the anion, and F is the Faraday constant. Using normalized (dimensionless) variables (cf. eq. (8) below), eq. (1) can be expressed as

$$R(T) = \int_0^1 \frac{dX}{C(X,T)} \tag{3}$$

where $X = x/\delta$, $T = tD/\delta^2$, $C(X, T) = c(X, T)/c_1$ and $R(T) = r(T)\lambda c_1/\delta$.

Changes in the convection velocity $v = v(t)$ will distort the concentration profile and thus cause a relaxation of the membrane resistance. In Teorell's membrane oscillator (1, 2, 5) the current is usually constant and the variation in the potential will be proportional to the resistance changes. To simplify the theoretical interpretation of the oscillator, Teorell (2) used an approximation for the non-steady-state behaviour of the resistance corresponding to the following equation:

$$\frac{dR(T)}{dT} = -K[R(T) - R(\infty)] \tag{4}$$

where $R(\infty)$ is the normalized steady-state membrane resistance at infinite time for constant convection velocity v and K is a constant. If $R(\infty)$ is time-independent, then the solution of eq. (4) is

$$R(T) = [R(0) - R(\infty)] \exp(-KT) + R(\infty) \tag{5}$$

where $R(0)$ is the initial steady-state resistance. The time constant (not normalized) of this approximation can be written as

$$\tau = \delta^2/KD = 1/k \tag{6}$$

where k is the rate constant used by Teorell in his

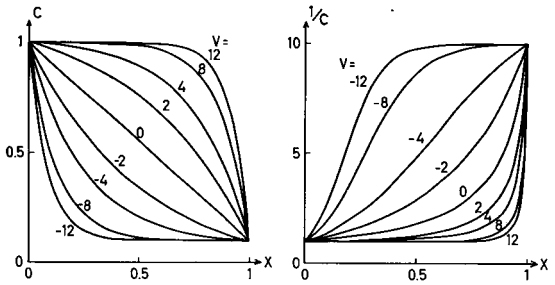

Fig. 3. Steady-state concentration profiles (left-hand figure) and resistivity profiles (right-hand figure) for the convection-diffusion model in Fig. 1, when $C_2 = c_2/c_1 = 0.1$. V is the normalized convection velocity defined as $V = v\delta/D$. Integration over the membrane of the resistivity profiles in the right-hand figure gives the normalized steady-state resistance R (∞) of the membrane.

approximation of the resistance-decay function corresponding to eq. (4).

In the present paper the exact variation of $R(T)$ has been calculated for a *step variation in the convection velocity* $v(t)$ from v_1 to v_2 (Fig. 2). The resistance maintains a steady-state value corresponding to the velocity v_1 at $t < 0$. The velocity is changed instantaneously and is kept constant at the new value v_2 at $t \geq 0$. The exact solution of $R(T)$ has been compared with the approximation in eq. (5).

The concentration $c(x, t)$ in the membrane is described by the following differential equation, derived from the equation of the solute flux through the membrane and the equation of continuity:

$$\frac{\partial c(x,t)}{\partial t} = D\frac{\partial^2 c(x,t)}{\partial x^2} - v(t)\frac{\partial c(x,t)}{\partial x} \qquad (7)$$

With normalized variables, eq. (7) can be rewritten (see normalizations under eq. (3)) as

$$\frac{\partial C(X,T)}{\partial T} = \frac{\partial^2 C(X,T)}{\partial X^2} - V(T)\frac{\partial C(X,T)}{\partial X} \qquad (8)$$

where $V(T) = v(T)\delta/D$.

The partial differential equation (8) is non-linear with respect to $V(T)$ and it is probably not possible to find an analytical solution for a general case. However, for a step-function variation of the convection velocity according to Fig. 2, an analytical solution in the form of a Fourier series can be found, as shown in the Appendix. This solution has been used in combination with eq. (3) to obtain the transient behaviour of the membrane resistance due to the velocity step.

COMPUTATIONS

Numerical solutions were obtained, using a Control Data 3 600 digital computer.

The *steady-state concentration profile* $C(X, \infty)$ and the corresponding resistivity profile, defined as $1/C(X, \infty)$, are shown in Fig. 3. The curves were calculated from eq. (A8) for different values of V. In this figure, as well as in all of the following calculations, $C_2 = 0.1$ was used.

The non-steady-state concentration $C(X, T)$ was calculated from eqs. (A7)–(A9). The sum was calculated by an iterative method. The summation was carried on until an iteration added to $C(X, T)$ a term which was less than $C(X, T) \cdot \sin(n\pi X) \cdot 10^{-6}$. A check was made that the addition of further terms did not alter the results in the significant figures. The transient resistance was calculated for each value of T from eq. (3) by means of Simpson's integration formula. Since the integration is most critical in the region near $X = 1$ for high values of V (see Fig. 3), a smaller size of the intervals was chosen in the region $X = 0.9 - 1$, as compared with $X = 0 - 0.9$ Usually 20 intervals were used for $X = 0 - 0.9$ and 40 intervals for $X = 0.9 - 1$.

RESULTS

Resistance response

The membrane resistance $R(T)$ was calculated for some different types of the *convection-velocity step*

$V(T) = V_1 \rightarrow V_2$							$\{V_m\}\,\Delta V$
V_1	$=0$	<0	$=0$	>0	<0	>0	$(V_m - \Delta V/2) \gtrless 0$
V_2	>0	$-V_1$	<0	$-V_1$	$=0$	$=0$	$(V_m + \Delta V/2) \gtrless 0$
Linear scale	Fig. 5	Fig. 6	Fig. 5	Fig. 7	Fig. 8	Fig. 8	–
Log scale	Fig. 9	Fig. 10	Fig. 11	Fig. 12	Fig. 13	Fig. 14	Fig. 15

Fig. 4. Classification of the different kinds of convection-velocity step functions $V(T)$ used in the calculation of the resistance response in the convection-diffusion model. The numbers of the figures, showing the results for the different cases, are also indicated.

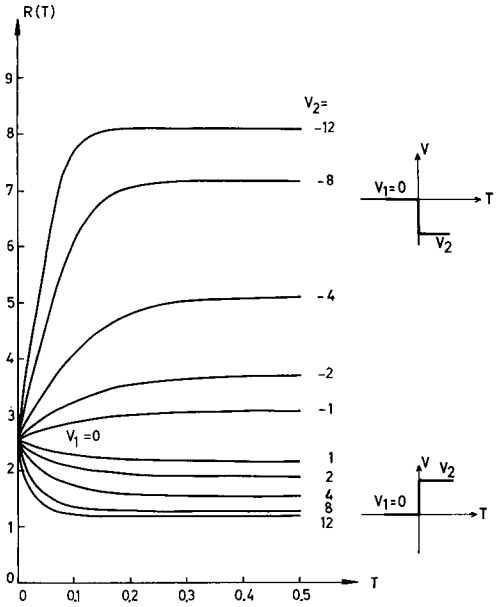

Fig. 5. The membrane resistance $R(T)$ as a function of time T for step changes in the convection velocity V from $V_1 = 0$ to positive and negative values of V_2 (cf. Fig. 4). Note that the time constant decreases as the step is increased. It will also be seen that the initial rise is steeper than exponential, when the step is high and negative.

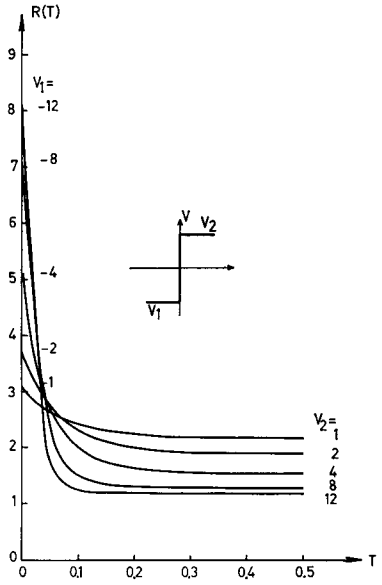

Fig. 6. Same as Fig. 5, but for positive velocity steps, which are symmetrical around $V = 0$ (cf. Fig. 4).

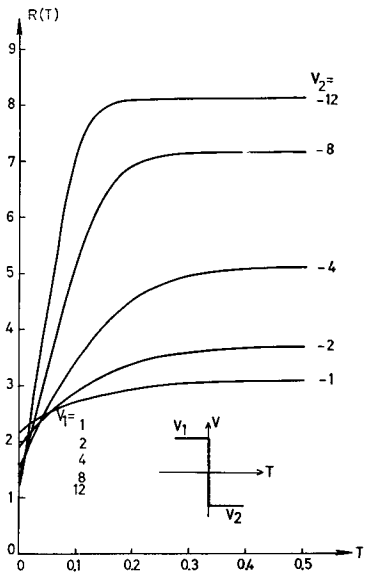

Fig. 7. Same as Fig. 5, but for negative symmetrical velocity steps (cf. Fig. 4).

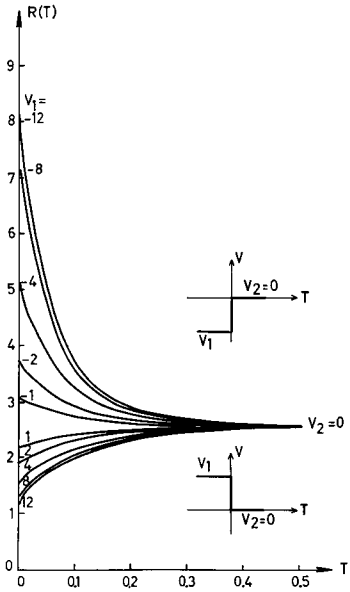

Fig. 8. Same as Fig. 5, but for positive and negative velocity steps to $V_2 = 0$ (cf. Fig. 4).

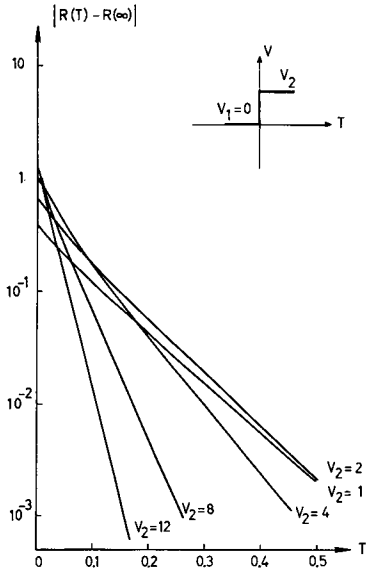

Fig. 9. The time-dependent deviation of the instantaneous resistance $R(T)$ from the final steady-state value $R(\infty)$ on a logarithmic scale in response to a positive step in the velocity V from $V_1 = 0$. (The same case is shown in Fig. 5.)

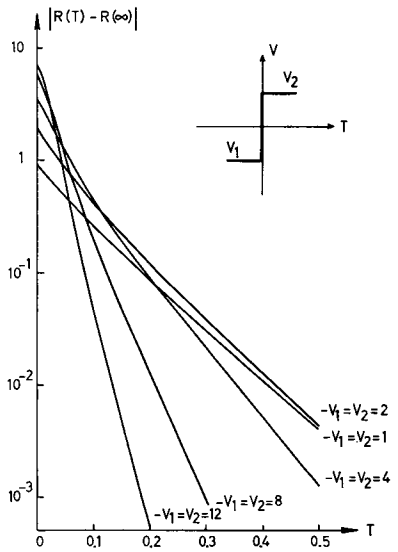

Fig. 10. Same as Fig. 9, but for a case corresponding to Fig. 6. Note the general resemblance, as compared with the curves in Fig. 9, which were calculated for the same V_2 values. The slopes approximate to identical values, with increasing T when the V_2 values are the same.

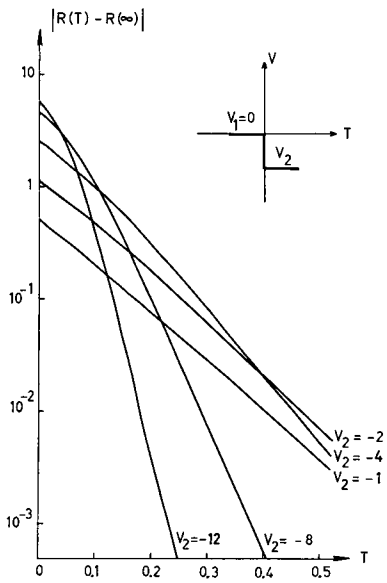

Fig. 11. Same as Fig. 9, but for a case also shown in Fig. 5.

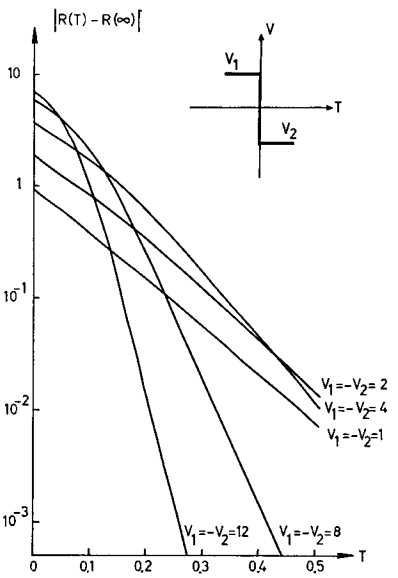

Fig. 12. Same as Fig. 9, but for the case also shown in Fig. 7. Note the resemblance to Fig. 11.

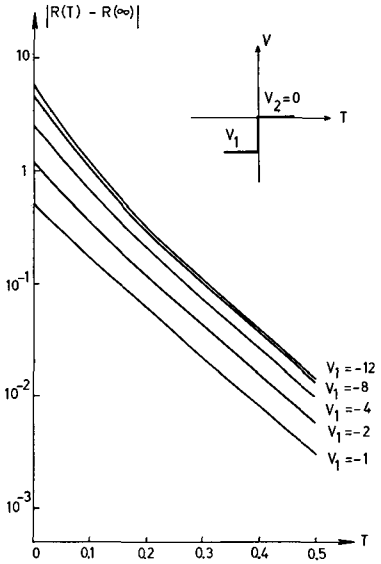

Fig. 13. Same as Fig. 9, but for a case also shown in Fig. 8.

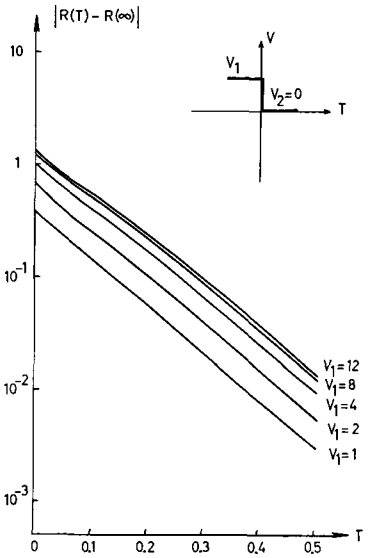

Fig. 14. Same as Fig. 9, but for a case also shown in Fig. 8. Compare with Fig. 13 and note that the curves in both figures are almost parallel, since V_2 has the same value ($V_2=0$) for all the curves.

function $V(T)$, which are *classified in Fig. 4.* The results are shown in Figs. 5–15, as indicated in Fig. 4. Figs. 5–8 give the resistance $R(T)$ on a linear scale as a function of the time T and in Figs. 9–15 the absolute value of the deviation of the resistance from the final steady-state value on a logarithmic scale is shown as a function of T. The velocity step function $V(T)$ used in Figs. 5–14 is defined as a step from an initial steady-state velocity V_1 at $T=0$ to a new velocity V_2. Three different classes of this type of velocity function can be distinguished from the alternatives shown in Fig. 4, namely, (1) positive or negative deviations from $V_1=0$, (2) positive or negative V_1 back to $V_2=0$ and (3) positive and negative steps centred around $V=0$. A more general definition of $V(T)$ is also adopted; it is defined as positive or negative steps ΔV centred around V_m (positive or negative). This latter definition is used in Fig. 15 for the case of small steps ($\Delta V=\pm 1$).

It will be seen from Figs. 5–15 that an *exponential approximation of* $R(T)$ *is not generally acceptable.* When the height of the step in V is below or equal to 4 (see Fig. 3 for the significance of this V value), the resistance curves are nearly straight lines in the logarithmic diagrams (Figs. 9–15). This means that the exponential approximation (eqs. (4) and (5)) is reasonable in this region. For higher values of the convection-velocity step, the logarithmic resistance variation is mostly convex upwards. On the linear scale the curves, which are upward convex on the logarithmic scale, show a steep, almost straight-line

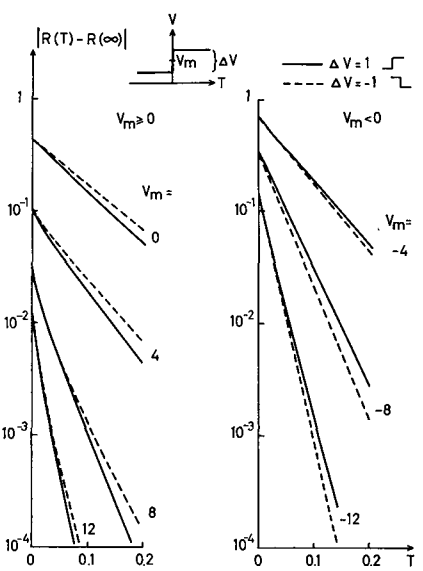

Fig. 15. Same as Fig. 9, but for a small step $\Delta V=\pm 1$ around a velocity V_m. Note that the curves are almost exponential, since the velocity step is small.

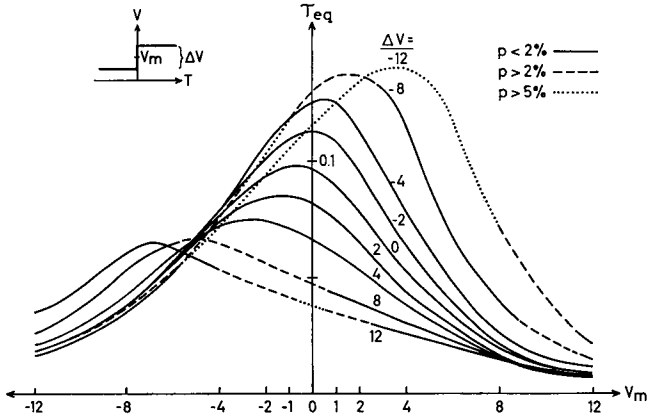

Fig. 16. Summary of the equivalent time constants τ_{eq} of the resistance relaxation as a function of the convection velocity step ΔV and the mean velocity V_m. τ_{eq} was calculated by fitting an exponential approximation to the exact time behaviour of the convection-diffusion resistance. The p values indicate different accuracies of the exponential approximation, as compared with the exact resistance (eq. (9)). If the curves are re-plotted with V_2 on the abscissa, then the maxima of τ_{eq} will fall approximately at $V_2 = -1$ to -2. The different heights of the maxima for different steps correspond to the different initial curvature in the $[R(T) - R(\infty)]$ plot.

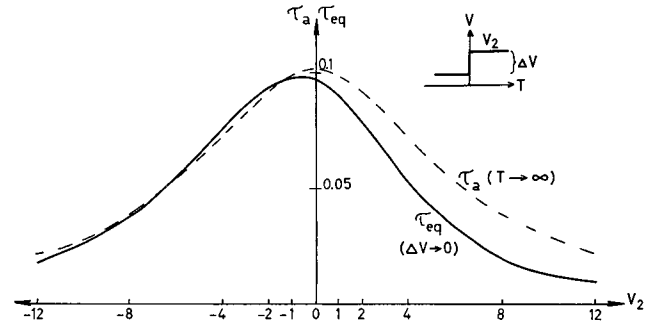

Fig. 17. The approximate time constant τ_a associated with large T values (dashed curve, from eq. (10)) and the equivalent time constant τ_{eq} for a small velocity step (continuous curve, taken from Fig. 16). The curve τ_a can be used as an approximation, suitable for analogue computations on Teorell's electrohydraulic excitability analogue.

rise initially (Figs. 5–7), with a small tendency to become sigmoid in some cases (Fig. 7).

It is striking that the resistance curves with different initial velocities V_1 but with the same final velocity V_2 show a general *resemblance*. This is quite obvious, if Figs. 9, 11 and 13 are compared with Figs. 10, 12 and 14 respectively. At high values of T the logarithmic curves approximate to identical slopes for each V_2 value independent of V_1. At small T values the principal behaviour is similar for curves with the same value of V_2.

Another important feature of the resistance curves (Figs. 5–15) is that the *time constant*, which is inversely related to the slope (K value) of the logarithmic curves, assumes a high value when V_2 is near zero, but is continuously reduced when V_2 is decreased or increased.

Numerical time constant

The exponential approximation of $R(T)$, according to eq. (5), has been tried in the following way. An equivalent time constant $\tau_{eq} = 1/K$ was introduced and defined as the time T when the absolute value of $[R(T) - R(\infty)]$ had decayed to $1/e$ of its initial value at $T=0$. This definition of τ_{eq} means that the exact $R(T)$ coincides at $T=1/K$ with the exponential approximation, according to eq. (5). As a measure of the accuracy of the approximation, the maximum relative deviation from the exact value of $R(T)$ was calculated according to the relation

$$p = \left| \frac{R(T)_{eq} - R(T)}{R(T)} \right|_{max} \qquad (9)$$

where $R(T)_{eq}$ is obtained from eq. (5), using $K = 1/\tau_{eq}$.

The results are shown in Fig. 16, where τ_{eq} is given as a function of V_m for a number of values of ΔV. The accuracy of the exponential approximation is indicated in the figure as approximate regions, where the p values are below 2%, between 2 and 5% or above 5%. It will be found from Fig. 16 that the exponential approximation is accurate within 2% when $|\Delta V| \lesssim 4$.

Theoretical time constant

A theoretical expression of the time constant at high values of T can be found from eq. (A7). The time behaviour of $C(X, T)$ is determined by a set of time constants equal to $1/[(V_2/2)^2+(n\pi)^2]$, one for each harmonic of order n (see eq. (A7)). For large T values, the time constant τ_a of the first harmonic will predominate, since higher harmonics have decayed. This means that

$$\tau_a = 1/[(V_2/2)^2+(\pi)^2] \text{ when } T\to\infty \qquad (10)$$

The time constant τ_a at large T is thus only dependent on the instantaneous convection velocity V_2. This property was also obvious from the numerical calculations, as discussed above.

The variation of τ_a with V_2 (eq. (10)) is shown in Fig. 17 (dashed curve), together with the τ_{eq} curve for small values of ΔV (continuous curve). The latter curve is identical with the curve for $\Delta V=0$ in Fig. 16. The two curves in Fig. 17 show a similar behaviour. This follows from the fact discussed above, that $R(T)$ is close to the exponential form for small steps (cf. Fig. 15), which means that the time constant τ_{eq} for small values of T in this case is approximately equal to the time constant τ_a at large T. For the special case that $V_2\to 0$ at the same time as $\Delta V\to 0$, the exponential approximation is almost exact, with a time constant according to eq. (10). This will be seen from eq. (A9), giving $a_2=0$ and $a_3/a_1=1/27$ under these conditions (see also Fig. 15).

It has also been shown by the present author (11) that a linearization of the convection-diffusion equations by a method used by Sandblom (12) yields a time constant close to the curves in Fig. 17. The linearization was accomplished by introducing a *sinusoidal* perturbation in V and the time constant was calculated as the inverse value of the characteristic frequency.

DISCUSSION

Conclusions

The following conclusions may be drawn from the results above, as regards the resistance variation due to a convection-velocity step.

1. The resistance relaxation is approximately exponential (accuracy within 2%) for steps in the velocity V which are less than or equal to 4.
2. The time-dependence of the resistance approaches the exact exponential form, if one of the following two conditions is fulfilled: (*a*) $T\to\infty$ or (*b*) $\Delta V\to 0$ and $V_2\to 0$.
3. The resistance–response curves for the same final velocity V_2 show a general resemblance, as regards the shape for small T and the logarithmic slope at higher T values.
4. The equivalent time constant is in general a non-linear function of V_2, with different values for positive and negative velocity steps.
5. When one of the conditions $\Delta V\to 0$ or $T\to\infty$ is valid, then the time constant may be approximated by eq. (10). In these cases the time constant is dependent on the value of V_2 but *not* on V_1.

Teorell's membrane oscillator

For a general case the resistance of the convection-diffusion model is non-linear, with a relaxational behaviour which is dependent not only on the instantaneous convection velocity but also on the previous history of the velocity. Thus, it is difficult or perhaps impossible to include a correct, simple description of the resistance relaxation in Teorell's equations, suitable for analogue computation. The approximation used by Teorell is an exponential resistance-delay function with a constant rate constant k. However, on the basis of the conclusions stated above, some possible modifications of Teorell's approximation will be discussed. Two different cases are considered.

1. *Free oscillations.* For a free-running membrane oscillator, the discrepancy between the instantaneous and steady-state resistance mostly corresponds to values of ΔV approximately less than 5 (see Fig. 3 in ref. 2 and Fig. 15 in ref. 13). This means that an exponential approximation of $R(T)$, as used by Teorell, is adequate for this case. The rate constant, on the other hand, is a more complicated function in the convection-diffusion model. However, eq. (10) may be used as a reasonable compromise. Thus it is suggested that the rate constant k in Teorell's equations should be replaced by the following expression:

$$k = [(V/2)^2+\pi^2]D/\delta^2 \qquad (11)$$

where $V=v\delta/D$ is the *normalized* convection velocity and $k=KD/\delta^2$ is the *non-normalized* rate constant.

The introduction of eq. (11) will affect the waveform of the potential oscillations. Since the time constant corresponding to eq. (11) becomes smaller when the absolute V value increases (eq. (10) and Fig. 17), it is expected that the rise and the fall of the potential oscillations will be faster with the new approximation, as compared with Teorell's constant k approximation. However, actual analogue-computer simulations must be performed, in order to elucidate the importance of the new approximation.

2. *Voltage clamp.* When the electrohydraulic excitability analogue is subjected to a voltage clamp, the step variation in the convection velocity may be very high. For this case, the detailed non-linearities are described by the complete equations of the convection-diffusion model. It has been shown by the present author (8) that the non-linear behaviour of the convection-diffusion conductance conforms well to the process of sodium activation in Hodgkin & Huxley's mathematical description of the giant axon (15).

APPENDIX

Analytical solution of the transient concentration

The solution of eq. (7) is found, using the following conditions (cf. Figs. 1 and 2):

Boundary conditions

(1) $c(o, t) = c_1 = \text{constant.}$
(2) $c(\delta, t) = c_2 = \text{constant.}$

Initial conditions

(3) $c(x, o) = \dfrac{\exp(v_1 x/D) - \exp(v_1 \delta/D)}{1 - \exp(v_1 \delta/D)} (c_1 - c_2) + c_2$
(4) $v = v_1, \quad \text{when } t < 0$

Input condition

(5) $v = v_2, \quad \text{when } t \geqslant 0$ (A1)

The initial condition (3) is the steady-state concentration profile (17, 2), when $v = v_1$, which is easily calculated from eq. (7) with $\partial/\partial t = 0$, together with the boundary conditions (1) and (2).

The partial differential equation (7) can be solved, using a transformation given by Fürth (14):

$$c(x, t) = c^*(x, t) \exp(vx/2D - v^2 t/4D) \tag{A2}$$

The transformation eq. (A2) applied to eq. (7) gives

$$\frac{\partial c^*(x, t)}{\partial t} = D \frac{\partial^2 c^*(x, t)}{\partial x^2} \tag{A3}$$

The transformed *boundary and initial conditions* eq. (A1) are

(1) $c^*(o, t) = c_1 \exp(v_2^2 t/4D), \quad \text{when } t \geqslant 0$
(2) $c^*(\delta, t) = c_2 \exp(-v_2 \delta/2D + v_2^2 t/4D),$

when $t \geqslant 0$

$$(3)\ c^*(x, o) = \left[\frac{\exp(v_1 x/D) - \exp(v_1 \delta/D)}{1 - \exp(v_1 \delta/D)} (c_1 - c_2) + c_2\right] \times \exp(-v_2 x/2D). \tag{A4}$$

Eq. (A3) has the same form as the equation of linear flow of heat. The general analytical solution for $t \geqslant 0$ of eq. (A3) with time-varying boundary conditions and an initial condition which is a function of x has been given by Carslaw & Jaeger (16) in the form of a Fourier series:

$$c^*(x, t) = \frac{2}{\delta} \sum_1^\infty \exp(-Dn^2\pi^2 t/\delta^2) \sin(n\pi x/\delta) \times \left[\int_0^\delta c^*(\xi, o) \sin(n\pi\xi d/\delta) + (nD\pi/\delta) \times \int_0^{+} \exp(Dn^2\pi^2\lambda/\delta^2)\{c^*(o, \lambda) - (-1)^n c^*(\delta, \lambda)\} d\lambda\right] \tag{A5}$$

The integrals in eq. (A5) can be solved after the substitution of eq. (A4). Finally, $c(x, t)$ is calculated from eq. (A2), using the expression derived from eq. (A5). This has been done and the result is shown in eqs. (A7)–(A9). However, the following normalized variables will first be introduced:

$$V_1 = v_1\delta/D \quad C(X, T) = c(X, T)/c_1$$
$$V_2 = v_2\delta/D \quad C_2 = c_2/c_1$$
$$X = x/\delta \tag{A6}$$
$$T = tD/\delta^2$$

$$C(X, T)_{V_1 \to V_2} = C(X, \infty) + 2(1 - C_2) \frac{\exp(V_2 X/2)}{1 - \exp(V_1)} \times \exp[-(V_2/2)^2 T] \times \sum_1^\infty a_n \exp[-(n\pi)^2 T] \sin(n\pi X) \tag{A7}$$

where

$$C(X,\infty) = \frac{\exp(V_2 X) - \exp(V_2)}{1 - \exp(V_2)}(1 - C_2) + C_2$$

(steady-state concentration profile) (A8)

and

$$a_n = n\pi\left[\frac{1}{(V_1 - V_2/2)^2 + (n\pi)^2} - \frac{1}{(V_2/2)^2 + (n\pi)^2}\right] \times [1 - (-1)^n \exp(V_1 - V_2/2)]. \quad \text{(A9)}$$

Eqs. (A7)–(A9) are thus the solution of eq. (8). In order to calculate the transient resistance response, eqs. (A7)–(A9) were computed numerically and the results were substituted in eq. (3).

The principal form of the solution of eq. (7) has been given by Cole (9) for a single-ion constant-field electrodiffusion regime, which is analogous to the convection-diffusion system considered here. The analogy is established if v is replaced by uFE, where u is the ion mobility, F the Faraday constant and E the electric field.

ACKNOWLEDGMENT

The author is greatly indebted to Professor T. Teorell for proposing this investigation and for numerous helpful discussions.

This work was financially supported by the Medical Faculty of the University of Uppsala, the Swedish Medical Research Council (Project No. 14X-629) and the National Institutes of Health (Grant No. 5, R01, HE12960-08).

REFERENCES

1. Teorell, T.: J Gen Physiol *42:* 831, 1959.
2. Teorell, T.: J Gen Physiol *42:* 847, 1959.
3. Kobatake, Y. & Fujita, H.: J Chem Phys *40:* 2219, 1964.
4. Aranow, R.: Proc Nat Abad Sci *50:* 1066, 1963.
5. Caplan, S. R. & Mikulecky, D. C.: *In* Ion Exchange (ed. J. A. Marinsky), vol. 1, p. 1. Marcel Dekker, Inc., New York, 1966.
6. Teorell, T.: *In* Handbook of Sensory Physiology (ed. W. R. Loewenstein), vol. I, p. 291. Springer-Verlag, Berlin, Heidelberg and New York, 1971.
7. Aranow, R.: Personal communication to T. Teorell.
8. Hägglund, J. V.: Upsala J Med Sci *77:* 77–90, 1972.
9. Cole, K. S.: Physiol Rev *45:* 340, 1965.
10. Labes, R.: Z Biol *93:* 42, 1932.
11. Hägglund, J. V.: unpublished results.
12. Sandblom, J.: Biophys J, in press, 1972.
13. Teorell, T.: Biophys J *2:* Part 2 (Suppl.), 27, 1962.
14. Fürth, R.: *In* Handbuch physik techn Mechanik (ed. F. Auerbach and W. Hort), vol. 7, p. 635, Leipzig, 1931.
15. Hodgkin, A. L. & Huxley, A. F.: J Physiol *117:* 500, 1952.
16. Carslaw, H. S. & Jaeger, J. C.: Conduction of Heat in Solids. Oxford University Press, 1959.
17. Manegold, E. & Solf, K.: Kolloid-Z *59:* 179, 1932.

Received February 24, 1972

Address for reprints:

Jarl Hägglund, BM
Institute of Physiology and Medical Biophysics
Biomedical Centre, Box 572
S-751 23 Uppsala
Sweden